



PARAMETERS INFLUENCING RESPONSE OF A BASE ISOLATED BUILDING

Ounis Hadj Mohamed*¹ and Ounis Abdelhafid²

¹Institute of Civil Engineering and Architecture, University of Batna, Algeria.

²Department of Civil Engineering, University of Biskra, 07000 Algeria.

Received: 10 June 2012; **Accepted:** 22 April 2013

ABSTRACT

In order to illustrate the effect of damping on the response of a base-isolated building, a large investigation is made. It consists in a parametric study which takes into account the progressive variation of the damping ratio (10% to 30%) under different nature of seismic excitations (near and far field). A time history analysis is used to determine a response of the structure represented in this case by terms of relative displacements and inter-stories drift at various levels of the building, additionally a strong deviation of energy capacity by the LRB (Lead Rubber Bearing) system will be recorded, therefore the results show that the efficiency of the isolator increases with the assumed damping ratio, provided that this latter is less or equal to 20%. Beyond this value, the isolator becomes less convenient.

Keywords: Damping; base isolation; LRB; seismic excitation; hysteresis; energy dissipation.

1. INTRODUCTION

In civil engineering, the main worry of the researchers is to reduce the damage caused by earthquakes on structures. In this context, it has been proven that mounting structures on base isolation is an important design strategy for protecting buildings from earthquake strong motions [1].

In this technique, a portion of the structure is isolated from the complete intensity of the seismic excitation and a great quantity of energy is dissipated using specific artificial techniques [2].

A significant investigation in the development of new methods of seismic resistant design has been carried out in New Zealand [Skinner 1975, 1976, 1982, 1984]; leading to the well-

*E-mail address of the corresponding author: hadjmohamed.ounis@univ-batna.dz (Ounis. Hadj Mohamed)

known "Laminated Rubber Bearing". These new isolation concepts, with a cylindrical plug of lead in central hole, were developed in the late 1970's [Robinson 1977], as it was experienced that the inherent damping in the rubber compounds available in Australasia at that time was inadequate to control the displacements of the isolation system [3].

The main use of the lead central part is to reduce the lateral displacement and offer an additional mechanism for energy dissipation, whereas the rubber bearing increases the flexibility and restoring force [4].

This fact reduces inertial forces and accelerations several times in the structure, but the additional flexibility due to the first natural period induces large displacement at the isolation level. So, this latter must be reduced to a tolerable level by energy dissipation using external dampers or introducing damping in bearing itself, that is wanted to maintain the isolator displacement inside acceptable limits in case of low frequency ground motion. Kelly [3] and Buckle and Mayes [6] carried out an extensive review on the historical developments of the many mechanisms that have been developed. While Bhasker, Rao and Jangid [7] conducted experimental and analytical study on the base-isolated structure having only one lateral degree of freedom with lumped mass system, Tsai and Kelly [8] extended this study to greatly damped base-isolated shear building with lumped mass system, leading to the following result: increasing the isolation damping will enlarge the super-structure acceleration with lumped mass system subjected to stationary random excitation, providing that the damping ratio of the isolation system remains beyond some level.

Seismic isolation for multistory buildings has been well evaluated and reviewed (Hong and Kim [12]; Barata and Corbi [13]; Agarwal [14]; Komodros [15] Lu and Lin [16]; Spyarakos [17]; Panayiotis et al [18]; Islam et al. a et b [19]. Base isolator with hardening behavior under increasing load has been developed for medium rise buildings (up to four storeys) and sites with moderate earthquake risk (Pocanshi and Phocas) [20]. Nonlinear seismic response evaluation was performed by Balkaya and Kalkan [21]. Resonant behavior of base isolated high rise building under long period ground motions was dealt by Ariga et al. [22] and long period ground motions building responses by Olsen et al. [23]. Wilkinson and Hiley [24] presented a nonlinear response history model for the seismic analysis of high rise framed buildings.

A nonlinear analysis of different parameters affecting the response of a structure with LRB isolation has permitted to determine the key parameters for an optimum conception of a LRB isolator. It consists of a very extensive parametric study which takes into account an incremental variation of the damping ratio. The optimal value of this latter is searched for under different types of seismic records: near fault records as those of the Lexington, Sylmarff and Elcentro stations and moderate excitation records as those of Oakwhaf station.

Other parameters proved to be necessary to the realistic understanding of the isolator behavior, particularly the proportion of the predominant seismic excitation frequency to the natural frequency of the superstructure.

Thus, a pursue investigation shows the efficiency of the LRB system mainly based on its capacity of energy absorption and dissipation according to the damping ratio

2. MODELING OF THE LRB SYSTEM

These systems exploit the principle of the laminated bearing and its lateral flexibility. The LRB isolation system is similar to a laminated rubber bearing with a central hole into which the lead core is press-fitted as shown in Figure 1. The core of lead is used to provide additional energy dissipation which significantly reduces lateral displacements. The system becomes essentially a damper hysteresis device. The force deformation characteristics of the hysteretic damper can be modeled exactly by a set of coupled non-linear differential equations. Typical hysteresis loops, such as elastic-plastic, rigid friction, bi-linear and smooth hysteretic, are generated by attributing appropriate values to the variables of the differential equation. [4].

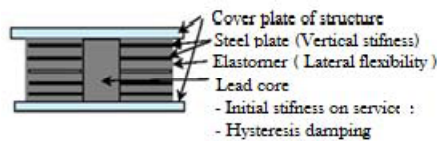


Figure 1. Components of the LRB system

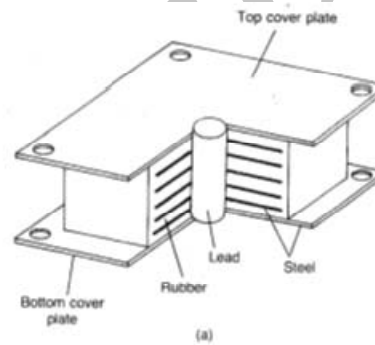


Figure 2(a). Lead rubber bearing

The LRB system is shown in figure 2(a), the schematic model is represented by figure 2(b) and the force-deformation behavior is illustrated in figure 2(c).

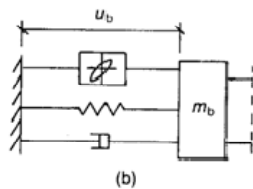


Figure 2(b). Mathematical model of the LRB system

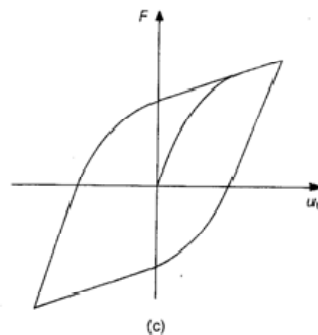


Figure 2(c). Hysteresis loop force-deformation for the LRB system

3. MODELING OF THE BASE-ISOLATED BUILDING

For the present study, the idealized mathematical model of the N story structure is shown in Figure 3.a. The base-isolated building is modeled as a shear type structure mounted on

isolation systems with two lateral degrees-of-freedom at each floor.

The following assumptions are made for the structural system under consideration:

During the earthquake excitation, the superstructure is considered to remain within the elastic limit. This assumption is valid in the presence of the isolator which reduces the response of the structure considerably.

The floors are assumed to be rigid in their planes and the mass is supposed to be lumped at each floor level.

The columns are inextensible and weightless, and provide the lateral stiffness.

The system is subjected to two horizontal components of the earthquake ground motion.

The effects of soil-structure interaction are not taken into consideration.

At each floor and base mass one lateral dynamic degree-of-freedom is considered. Therefore, for the N-storey superstructure the dynamic degrees-of-freedom are $N + 1$.

The governing equations of motion for the N-stories superstructure model are expressed in matrix form as:

$$[M]\{\ddot{x}\} + [C]\{\dot{x}\} + [K]\{x\} = -[M]\{1\}(\ddot{x}_b + \ddot{x}_g) \quad (1)$$

Where $[M]$, $[C]$, $[K]$, are, respectively, the mass, damping, and stiffness matrices of the fixed base of the order $N \times N$.

$\{x\} = \{x_1, x_2, x_3, \dots, x_n\}^T$, is the displacement of the superstructure; $x_j = (j = 1, 2, \dots, N)$, is the lateral displacement of the j th floor relative to the base mass; $\{1\} = \{1, 1, 1, \dots, 1\}^T$ is the influence coefficient vector; $\{x\}$, $\{\dot{x}\}$, and $\{\ddot{x}\}$, are the unknown relative floor displacement, velocity, and acceleration vectors, respectively.

\ddot{x}_b , and \ddot{x}_g are the relative acceleration of the base mass and earthquake ground acceleration, respectively.

The structural model of the isolated building is represented in figure 3(a) as follows.

Figure 3(b) shows the Bilinear Hysteretic model for the LRB isolator.

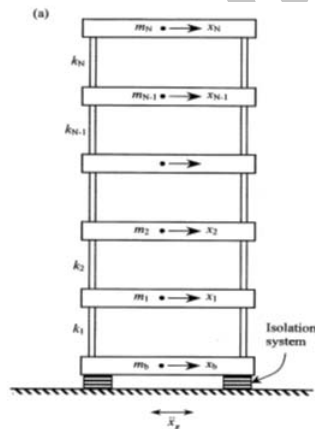


Figure 3(a). Mathematical model of the N-story base-isolated building

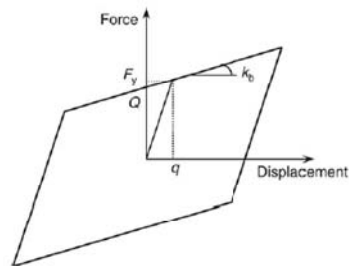


Figure 3(b). Bilinear hysteretic model of the LRB isolator

The corresponding equation of motion for the base mass under earthquake ground

acceleration is expressed by

$$m_b \ddot{x}_b + c_b \dot{x}_b + F_b - k_1 x_1 - c_1 \dot{x}_1 = -m_b \ddot{x}_g \quad (2)$$

Where m_b , is the mass of base raft; F_b : is the restoring force developed in the LRB isolation system,

k_1 : is the stiffness of the first floor of the superstructure;

c_1 : is the damping of the first story of the superstructure.

The restoring force developed in the isolation system F_b depends upon the type of isolation system considered and on the approximate numerical models used.

4. MATHEMATICAL MODEL OF THE LRB SYSTEM

For the present study, the force-deformation behavior of the isolator is modeled as nonlinear hysteretic represented by the bilinear model [25].

The nonlinear force-deformation behavior of the isolation system is modeled through the bilinear hysteresis loop characterized by three parameters namely; (i) characteristic strength, Q (ii) post-yield stiffness, k_b and (iii) yield displacement, q (refer Figure 3.b). The bilinear behavior is selected because this model can be used for all isolation systems used in practice. The characteristic strength, Q is related to the yield strength of the lead core in the elastomeric bearings and friction coefficient of the sliding type isolation system, k_b is generally designed in such a way to provide the specific value of the isolation period, T_b expressed as

$$T_b = 2\pi \sqrt{\frac{M}{k_b}} \quad (3)$$

Where $M = (m_b + \sum_{j=1}^N m_j)$ is the total mass of the base-isolated structure of the j th floor of the superstructure.

The yield strength of the bearing is normalized with respect to the total weight of the isolated building and expressed by the parameter, F_0 defined as:

$$F_0 = \frac{F_y}{W} \quad (4)$$

Where $W = m \cdot g$ is the total weight of the isolated building; and g is the acceleration due to gravity.

The viscous damping, c_b in the bearing due to rubber is evaluated by the damping ratio, ξ_b expressed as:

$$\xi_b = \frac{c_b}{2m\omega_b} \quad (5)$$

Where $\omega_b = 2\pi/T_b$ is the base isolation frequency.

Thus, the modeling of LRB requires the specification of four parameters namely the isolation period (T_b), damping ratio (ξ_b), normalized yield strength F_0 and yield displacement (q).

5. SOLUTION OF MOTION EQUATIONS

In this situation the Classical Modal Superposition technique cannot be employed in the solution of equations of motion here because.

The system is non-classically damped because of the difference in damping in the isolation system and in the superstructure.

The force-deformation behavior in the considered isolation systems is non-linear.

Therefore, the equations of motion are solved numerically using Newmark's method of step-by-step integration; adopting linear variation of acceleration over a small time interval of Δt . The time interval for solving the equations of motion is taken as 0.02/200 s (i.e. $\Delta t = 0.0001$ s).

6. PARAMETRIC STUDY

To illustrate the effect of damping on the response of a building with base isolation an extensive investigation was undertaken, a building of reinforced concrete of ten stories with a regular in plan and elevation of 15×20 m is considered with four spans in the longitudinal direction and three spans in the transverse direction placed 5 m apart. Sections of the beams are 30×45 cm², sections of the columns are 50×50 cm² and the floor height is 3 m with solid slabs 20 cm thick.

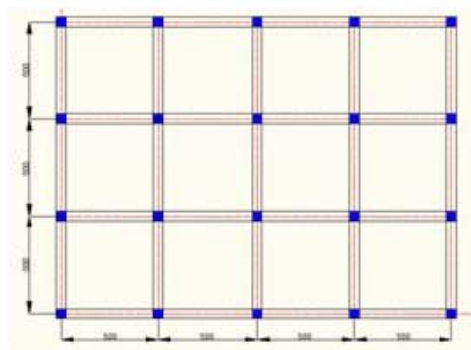
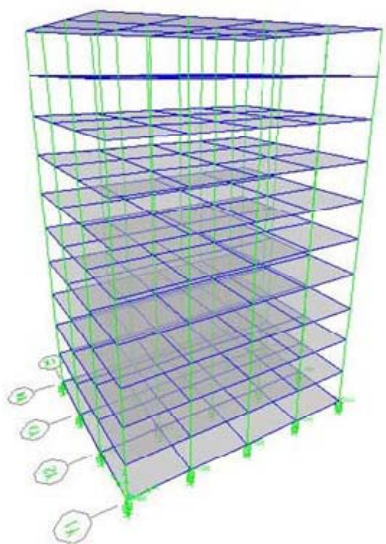


Figure 4(a). 3D view of the isolated structure Figure 4(b). Plan view of the isolated structure

The seismic excitations considered in this study are:

- Component of El Centro Imperial Valley earthquake (1979),
 - Component Outer Harbor Wharf in Oakland Loma Prieta Earthquake (1989),
 - The component of Lexington Dam Loma Prieta Earthquake (1989),
 - The component of Sylmar County Northridge Earthquake (1994),
- with Peak Ground Acceleration(PGA) 0.436 g, 0.287 g, 0.442 g and 0.604 g respectively.

The frequency analysis of these accelerograms showed that the frequency ranges of the seismic excitations are distributed as follows:

- Component of El Centro Imperial Valley: 0.15 to 0.5Hz.
- Component Outer Harbor Wharf in Oakland Loma Prieta: 0.5 to 1.65Hz.
- The component of Lexington Dam Loma Prieta: 0.65 to 2.45Hz.
- Component of Northridge Sylmar County: 0.35 to 3.6Hz.

The numerical simulation was run using ETABS V9.7.2 software, which is produced by the firm Computers and Structures, University of Berkley, USA.

7. RESULTS

7.1 Relative displacement

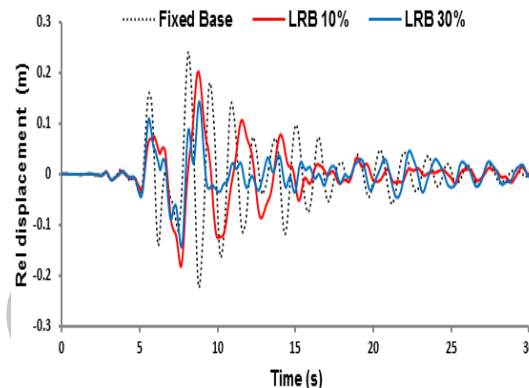


Figure 5. Comparison of relative displacement of top level between fixed base and base isolated with low (10%) and high (30%) effective damping ratios subjected to the component of El Centro Imperial Valley Earthquake.

The curves in Figure 5, resulting from the excitation of Elcentro for a conventional building and a base isolated building of type LRB, show a reduction of the relative displacement of floor of (16.05 and 39.98 %) for a damping ratio of (10% and 30%) respectively. Thus energy dissipation seems less promising specifically for this excitation on the one hand, and there is a strong proportionality between the reduction of displacement and the damping ratio on the other hand.

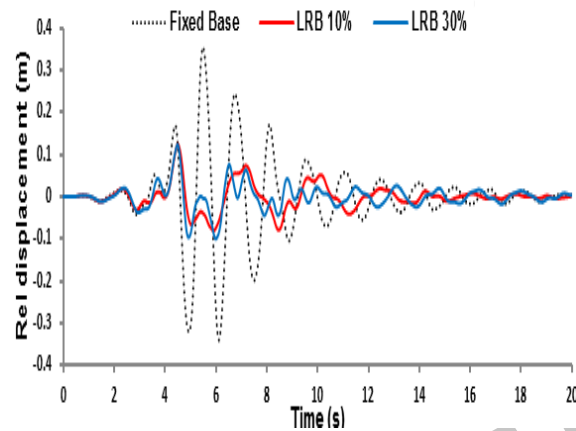


Figure 6. Comparison of relative displacement of top level between fixed base and base isolated with low (10%) and high (30%) effective damping ratios subjected to the component of Lexington Dam Loma Prieta earthquake.

From these curves obtained by the component of Lexington, we deduce that there is a strong energy dissipation by the isolation system which resulted in the reduction of the relative displacement of the floor with a very high ratio (64.91 and 65.25%) for a damping ratio of (10 and 30%, respectively). We also observe, that the increase in the damping ratio is insignificant for this type of excitation as the reduction of the displacement is nearly constant.

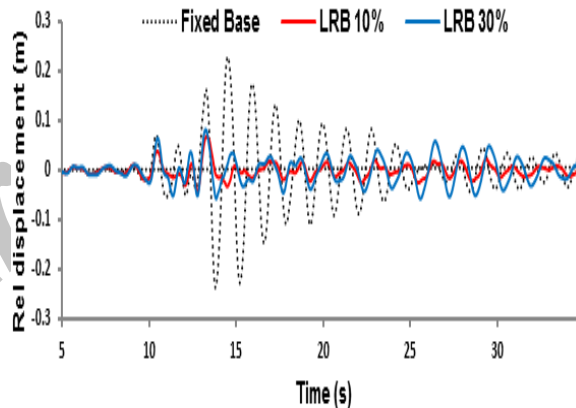


Figure 7. Comparison of relative displacement of top level between fixed base and base isolated with low (10%) and high (30%) effective damping ratios subjected to the component of Oakland Outer Loma Prieta Earthquake.

Under the effect of the component of Oakland Outer Loma Prieta Earthquake, there was a deviation of almost all of the seismic energy to the LRB isolator, which resulted in to a strong reduction of the relative displacement estimated at Top (70.03 and 64.10%) under damping ratios of (10 and 30%), respectively, which makes the isolation system highly

efficient.

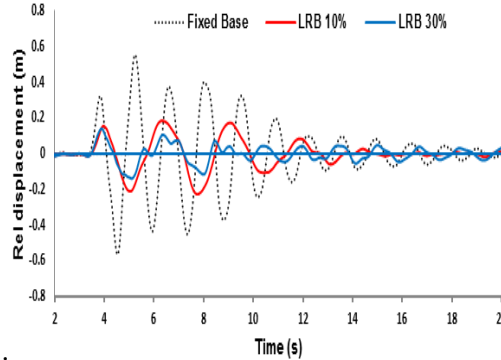


Figure 8. Comparison of relative displacement of top level between fixed base and base isolated with low (10%) and high (30%) effective damping ratios subjected to the component of Sylmar County Northridge earthquake.

The graph in Figure 8 shows that higher levels of the damping ratio of the isolator result in highly significant reduction in the relative displacement which imply that the base isolation is very effective for this excitation. The reduction of the relative displacement is estimated at (59.39 and 74.70%) for a damping ratio (10 and 30%) respectively.

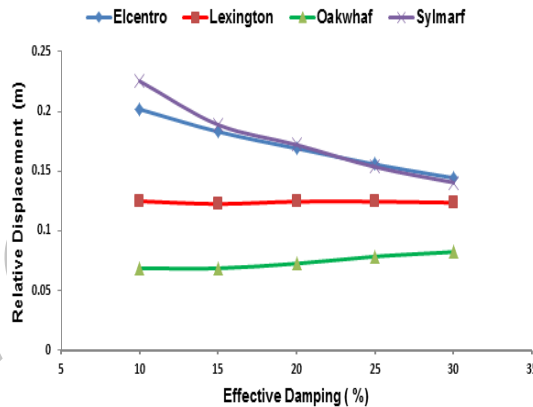


Figure 9. Maximum Relative Displacement of the Top level with different effective damping ratios subjected to the multitude seismic excitation

The graph shows the variation of the relative displacement Top Max as a function of the variation in the damping ratio for different seismic excitations, which suggests therefore it indicates that the LRB isolation system is effective because of the high reduction in the ratio of relative displacements which may exceed 74% with certain types of excitations. We observe for the excitations Sylmarff and Elcentro that the damping ratio is proportional of the relative displacements Top, which can reach 0.14 m. However for the excitation Oakwhaf and Lexington, there is almost a complete stagnation of the reduction of the relative displacement Top, thus, increasing the damping ratio of the isolator is not necessary, in

conclusion the LRB isolator is more effective for Oakwhaf excitation as reflected by a significant reduction in the Top relative displacement.

7.2 Inter-stories Drift

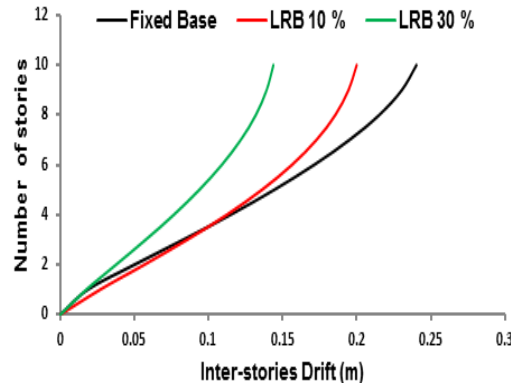


Figure 10. Comparison of inter-stories Drift between fixed base and base isolated with low (10%) and high (30%) effective damping ratios subjected to the component of El Centro Imperial Valley Earthquake.

The curves in Figure 10 result from a comparative study of the inter-story drift in a conventional building equipped with a LRB isolation base with damping ratios of 10 and 30%. For an Elcentro excitation, we recorded reductions of 16.79 and 40.16 in the inter-story floor-terrace displacements for damping ratios of 10 and 30%, respectively. Thus, while smaller reductions were observed for damping ratios of 10%; substantial reductions were observed for high damping rates (30%).

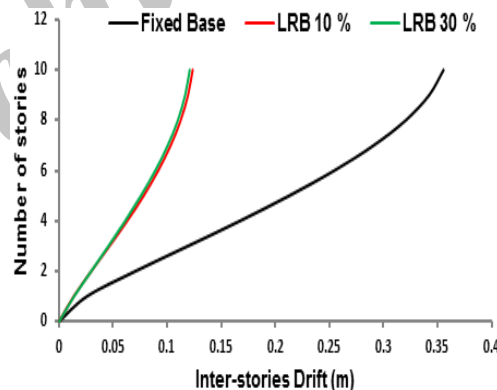


Figure 11. Comparison of inter-stories Drift between fixed base and base isolated with low (10%) and high (30%) effective damping ratios subjected to the component of Lexington Dam Loma Prieta earthquake.

For the excitation of Lexington, the inter-story drifts are estimated at 65.25 and 66.03% for damping ratios of 10 and 30%, respectively. Thus, on the one hand, we observe a strong

reduction in the inter-story drift reaching up to a level of 66%, which reflects the reliability of the LRB isolation system, we observe, on the other hand, that the two curves, corresponding to the damping ratios of 10 and 30%, are close to each other, thus, for technical and economic considerations, we limit ourselves to the LRB excitation system with a 10% ratio.

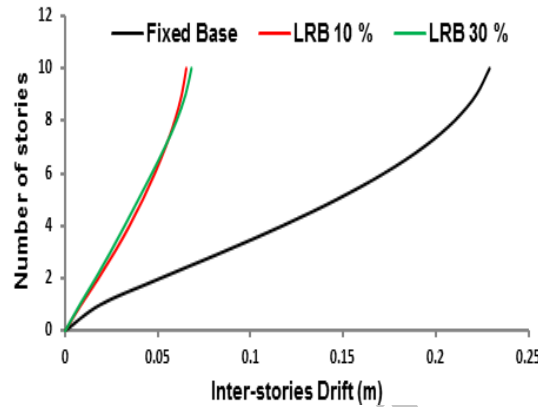


Figure 12. Comparison of inter-stories Drift between fixed base and base isolated with low (10%) and high (30%) effective damping ratios subjected to the component of Oakland Outer Loma Prieta Earthquake.

Results under the excitation Oakwhaf are practically the same as that of the excitation Lexington. They are characterized by a significant reduction of the inter-story drift, estimated at 71.43 and 70.23% for damping ratios of 10 and 30%, respectively. Therefore, the LRB isolation system with a 10% damping ratio is adequate in reducing the inter-story drift with an estimated reduction of 71.43% (0.0682 m).

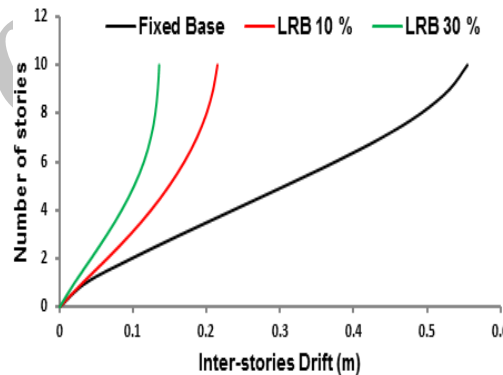


Figure 13. Comparison of inter-stories Drift between fixed base and base isolated with low (10%) and high (30%) effective damping ratios subjected to the component of Sylmar County Northridge earthquake.

Despite an excitation characterized by a high Pick Ground Acceleration PGA (0.604 g) of that of Sylmar County, the inter-stories drift is reduced proportionally to the damping ratio

of the isolator. The reduction in displacements is estimated at 61.28 and 75.57% for damping ratios of 10 and 30%, respectively. Therefore, the LRB isolation system is very effective in reducing the inter-story drift with reductions reaching up to 75% with a value of 0.1358 m.

7.3 Energy balance

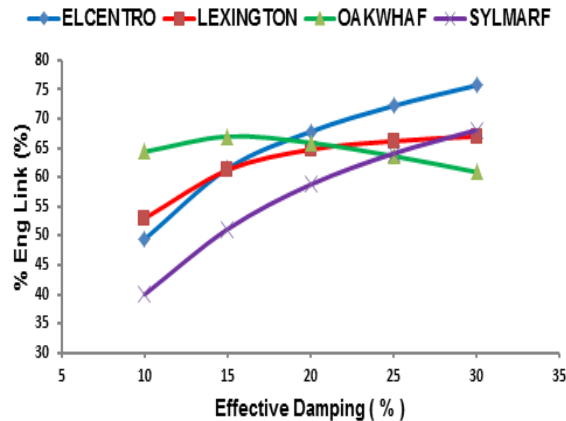


Figure 14. Maximum of the % Link Energy with different effective damping ratios subjected to the multitude seismic excitation.

When a structure is subjected to a strong earthquake the system energy of the structure can be expressed as follows: $IE = KE + PE + LE + MDE$

Where:

IE = Input Energy ; KE = Kinetic Energy

PE = Potential Energy ; LE = Link element Energy

MDE = Modal Damping Energy

The curves in figure14 represents the maximum percentage of link energy absorbed by the isolator according to its damping ratio under different seismic excitations with different nature (near, medium and free field), and different frequency content. Each curve corresponds to the analysis of a single excitation;

For the excitation of Elcentro, we observe that the energy absorbed by the isolator is proportional to the damping ratio but this variation is not perfectly linear. We also record a dissipation ratio of 49.43 and 75.73% for damping ratios of 10 and 30%, respectively. Therefore, the optimal value (technical-economic) can be achieved at a ratio of 20% (corresponding to 67.82% of Input Energy absorbed by the LRB isolation system).

According to the accelerogram LEXINGTON, we observe, at a 10% damping ratio, a slight increase in the dissipation of the input energy equal to 52.99% as compared to that of ELCENTRO. One can subdivide the curve into two parts, the first part is roughly increasing (between 10% and 20%), while the second part is slight monotonous. Therefore, the most appropriate damping ratio is 20% (corresponding to 64.75% of Input Energy absorbed by the LRB, which slightly lower than that of ELCENTRO).

According to the curve for the excitation OAKWHAF, the percentage of damping is

inversely proportional to the dissipation of Input Energy, specifically, dissipation decreases according to a curvilinear trend as the damping ratio increases. It is interesting to note that a strong dissipation of Input Energy is recorded (64.39%) for a damping ratio of 10% which is equivalent to dissipations under ELCENTRO and is even closer to that of a LEXINGTON ratio of 20%. Therefore, we opt for an isolation system with a damping ratio of 10% for this excitation.

Based on the accelerogram SYLMARF, we observe that the dissipation by the isolator is similar to that ELCENTRO, but with a lag almost uniformly estimated at 9%. The optimal value of the damping ratio is estimated at 20% which corresponds to an estimated dissipation of the Input Energy of 58.77%.

The curves in Figure 15 show the variation of the energy from modal damping of the superstructure based on the damping ratio of the isolator under diverse seismic excitations of different nature. We mainly observe that the evolution of energy from modal damping of the structure is determined symmetrically from the Link energy absorbed by the isolator. In other words, the two types of energy are inversely proportional, i.e., complementary.

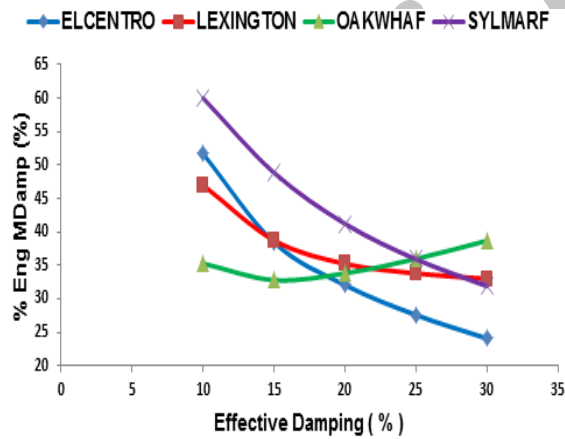
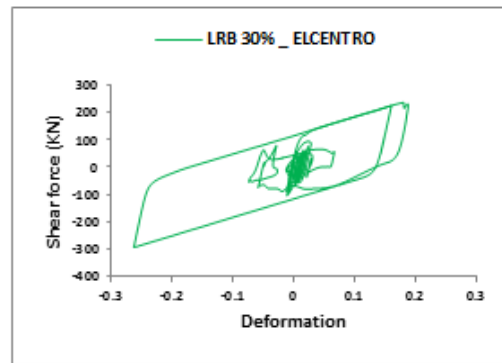
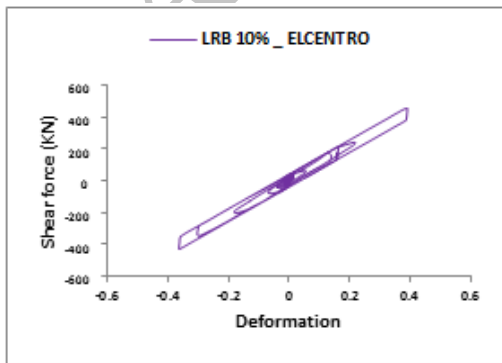


Figure 15. Maximum of the % MDamping Energy with different effective damping ratios subjected to the multitude seismic excitation

7.4 Energy absorbed by LRB System



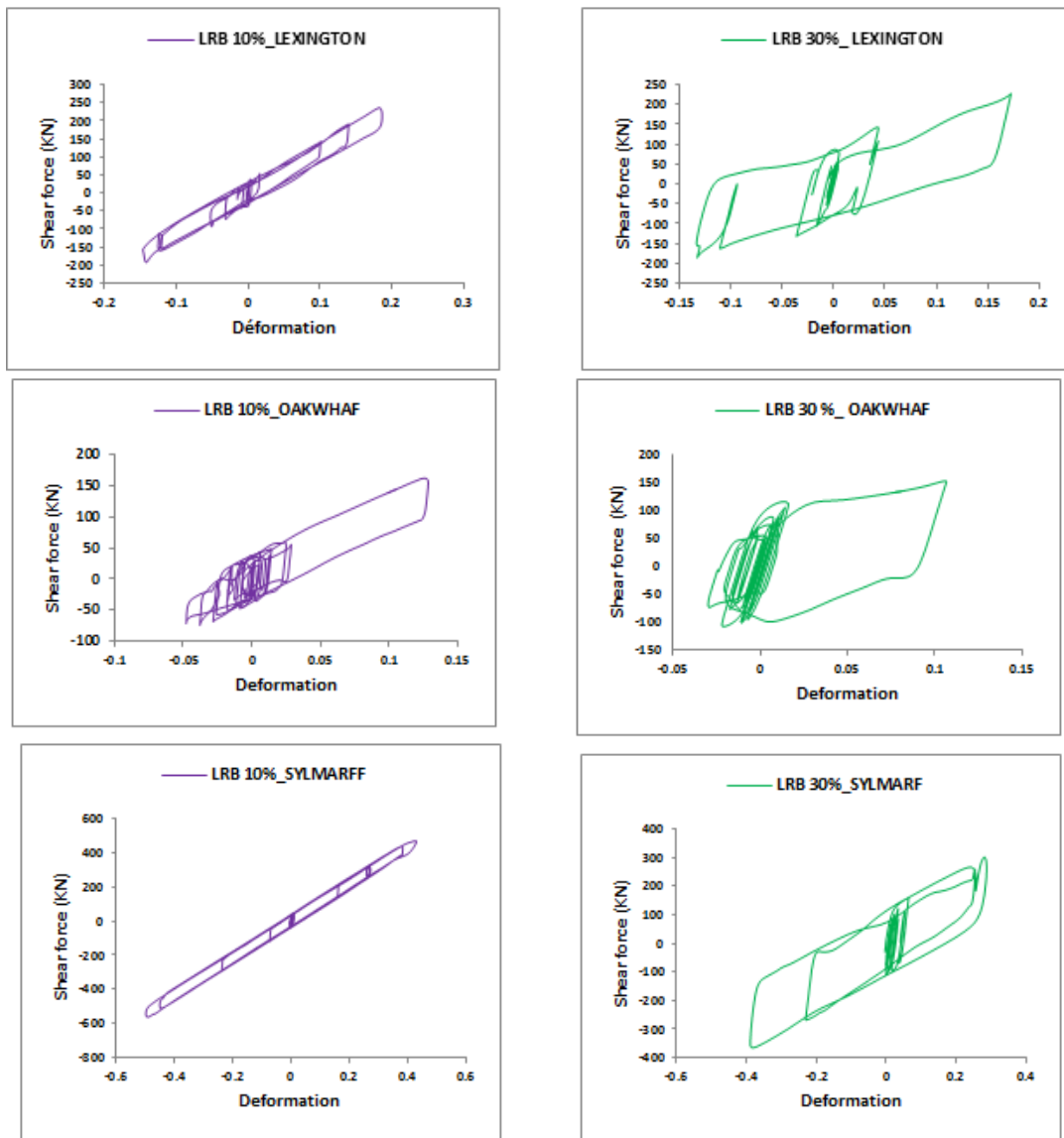


Figure 16. Hysteresis Loop Force-Deformation

Figure 16 includes a set of hysteresis curves describing the energy absorption capacity of the isolator at damping rates of 10 and 30% under four different types of excitations. We observe from the curves below that higher damping rates correspond to an increase in the surface of the hysteresis curve. This suggests the effectiveness of using the LRB system as reflected by a high absorption capacity of the seismic energy input.

8. CONCLUSION

This investigation concerns the comparison of a conventional building to a building with LRB based isolation, through a very broad parametric study. It aims to find the optimal characteristics of the isolation system LRB, subjected to different seismic excitations of different nature and different levels of damping rates of the LRB isolators (10-30%). This simulation yielded the following results:

The relative displacement of the floor to terrace is greatly reduced, at a rate of approximately 65% for all excitations except for that of Elcentro. Therefore, the LRB system is most appropriate at a damping rate of 20%.

We observe that the inter-story displacement depends mainly on the nature of the seismic excitation. The average displacement reduction is estimated at 40% for high damping rates under the Elcentro excitation; in contrast, there is a strong reduction of the inter-story displacement (65 and 70%) at a low damping rate (10%) under the excitations of Lexington and Oakwhaf, respectively. Moreover, we record for these two excitations a perfect coincidence of the two curves at different damping rates (10 and 30%). A high attenuation (estimated at 61%) was observed for the excitation of Sylmarff even at a low rate of depreciation (10%), even though this excitation is characterized by high PGA (0.604 g). Therefore, the LRB isolator with a low damping rate (10%) reduces the inter-story displacement, on average by 65%.

The isolator LRB plays a major role for which it has been designed, this results on the one hand by the increase in the surface of the hysteresis curve, and, on the other hand, by a high energy absorption estimated at an average rate of 65% for an optimum damping rate of 20%. This indicates the major effect of LRB isolator as an energy absorber.

The protection by base isolation depends on the fundamental frequency of the structure and the frequency domain of the seismic excitation. Therefore, the structural type of the building and the soil conditions in the site can affect the efficiency of the isolation system

The optimal design of system-based isolation LRB is controlled according to the ratio of the predominant frequency of soil (w_g) and the fundamental frequency of the superstructure (w_s), knowing that for small values of the ratio $\frac{w_g}{w_s}$ the system becomes less effective, which is the case of a flexible superstructure. In contrast, the LRB isolation system is more efficient when the ratio is close to unity

We note that the displacement at the base decreases when the ratio $\frac{w_g}{w_s}$ is increased; this means that the LRB isolator at the base is more suitable for structures with rigid foundation.

REFERENCES

1. Chung LL, Yang CY, Chen HM, Lu LY. Dynamic behavior of nonlinear rolling isolation system, *Structural Control Health Monitoring*, **16**(2009) 32-54.
2. Priestley MJN, Calvy GM. *Seismic Design and Retrofit of Bridges*, a Wiley International Publication, 1996.
3. Kelly JM. Seismic base isolation: review and bibliography, *Soil Dynamics Earthquake Engineering*, No. 3, **5**(1986) 202-16.

4. Kang BS, Kang GJ, Moon BY. Hole and lead plug effect on fiber reinforced elastomeric isolator for seismic isolation, *Journal of Material Processing Technology*, **140**(2003) 592-7.
5. Krishnamoorthy, Shetty KK. Effect of isolation damping on the response of base isolated structure, *Asian journal of civil engineering (Building and housing)*, No.10, **6**(2009) 701-16.
6. Buckle IG, Mayes RL. Seismic isolation: history, application and performance—A word overview, *Earthquake Spectra*, No. 2, **6**(1990) 161-202.
7. Bhasker R, Jangid RS. Experimental study of Base isolated Structures, *Journal of Earthquake Technology*, **38**(2001) 1-15.
8. Tsai HC, Kelly JM. Seismic response of heavily damped base isolation, *Systems Journal of Earthquake Engineering and Structural Dynamics*, **22**(1993) 633-45.
9. Jangid RS, DattaTK. Seismic behavior of base isolated buildings: a state of the art review, *Civil Engineering Structures & Buildings*, **110**(1995) 186-203.
10. DM Lee, IC Medlan. Base isolation systems for earthquake protection of multistorey shear structure, *Earthquake engineering and structural dynamics*, **7**(1979) 555-68.
11. Constantinou MC, Tadjbakhsh IG. Hysteretic dampers in base isolation: Random approach, *American Society for Civil Engineering*, No. 111, **4**(1985) 705-21.
12. Hong W, Kim H. Performance of a multi-storey structure with a resilient-friction base isolation system, *Computers & Structures*, **82**(2004) 2271-83.
13. Baratta A, Corbi I. Optimal design of base-isolators in multistorey buildings, *Computers & Structures*, **82**(2004) 2199-2209.
14. Agarwal VK, Niedzwecki JM, Van de Lindt JW. Earthquake induced pounding in friction varying base isolated buildings, *Engineering Structures*, **29**(2007) 2825-32.
15. Komodromos P. Simulation of the earthquake-induced pounding of seismically isolated buildings, *Computers & Structures*, **86**(2008) 618-26.
16. Lu LY, Lin GL. Predictive control of smart isolation system for precision equipment subjected to near-fault earthquakes, *Engineering Structures*, **30**(2008) 3045-64.
17. Spyrakos CC, Koutromanos IA, ManiatakisCA. Seismic response of base-isolated buildings including soil-structure interaction, *Soil Dynamics of Earthquake Engineering*, **29**(2009) 658-68.
18. Islam ABMS, Jameel M, Jumaat MZ. Seismic isolation in buildings to be a practical reality: Behaviour of structure and installation technique, *Journal of Engineering and Technology Research*, No.3, **4**(2011a) 97-117.
19. Islam ABMS, Ahmad SI, Jameel M, Jumaat MZ. Study on corollary of seismic base isolation system on buildings with soft story, *International Journal of the Physical Sciences*, No. 6, **9**(2011) 2219-28.
20. Pocanschi A, Phocas MC. Earthquake isolator with progressive nonlinear deformability, *Engineering Structures*, **29**(2007) 2586-92.
21. Balkaya C, Kalkan E. Nonlinear seismic response evaluation of tunnel form building structures, *Computers & Structures*, **81**(2003) 153-65.
22. Ariga T, Kanno Y, Takewaki I. Resonant behavior of base isolated high-rise buildings under long-period ground motions, *The Structural Design of Tall and Special Buildings*, **15**(2006) 325-38.
23. Olsen A, Aagaard B, Heaton T. Long-period building response to earthquakes in the

San Francisco Spans Area, *Bulletin of the Seismological Society of America*, No 2, **98**(2008) 1047- 65.

24. Wilkinson S, Hiley R. A non-linear response history model for the seismic analysis of high-rise framed buildings, *Computers & Structures*, **84**(2006) 318-29.
25. Vasant A.M, Jangid R.S. Influence of isolator characteristics on the response of base-isolated structures, *Engineering structures*, **26**(2004)1753-49

Archive of SID